

Reinforcement Soft Soil by Ballast and Geo Grid Overlaying the Soil

Ghufraan Mohammed About ,Mariam Hassan Abbas

Assistant lecture, department of highway and transportation engineering, Al-Mustansiriyah University
Assistant lecture, Ministry of education ,General Directorate of Education in Karbala
Iraq, Baghdad

Abstract

Eight models are performed with ballast layer reinforced with geogrid overlying the soft soil. These models are performed using different ballast thickness (H) of (25, 50, 75 and 100 mm). Four models are performed oneach of the two undrained shear strengths (9kPa) and (25kPa).

Initially, a single layer of geogrid is placed along the interface plane between the ballast and soft soil. when the ballast layer is increased from (25mm) to (50, 75, 100mm) ,the load capacity increases for about (28% and 58%) for models (SGB-7 and SGB-8) respectively. Also, when the ballast layer is increased from (50mm) to (75 and 100mm) the load capacity increased for about (28% and 58%) for models (SGB-7 and SGB-8) respectively. While, increasing the ballast layer from (75mm) to (100mm) leads to an increase in the load capacity for about (24%) for model (SGB-8).This means the value of undrained shear strengths and presence of geogrid under the ballast layers represent an important parameters to improve soil and as a result, the load capacity increased. Also, increasing the value of undrained shear strengths from (9kPa) to (25kPa) lead to increase (improve) the carrying capacity of soft soil and as a result, the load transferred by ballast decreased.

Keywords: soft soil ,ansys, ballast, undrained shear strength.

I. INTRODUCTION

To study more thoroughly the behavior of soft soil, with or without ballast and geogrid layers, a nonlinear finite element analysis has been carried out to analyze all adopted models. The analysis is performed by using the finite element models.

II. FAILURE CRITERIA FOR SOFT SOIL

yield criterion is widely used for finite element analysis of granular material problems (such as soil, gravel, sand, rocks. ..ect). In ANSYS program, the option uses the Drucker-Prager yield criterion is available with either an associated or non-associated flow rule. The yield surface does not change with progressive yielding, hence there is no hardening rule

and the material is elastic- plastic[1], Figure (1). The equivalent stress for **Drucker-Prager** is:

$$\sigma_e = 3 \beta \sigma_m + \left[\frac{1}{2} \{S\}^T \{M\} \{S\} \right]^{1/2}$$

where:

$$\sigma_m = \text{the mean or hydrostatic} = \frac{1}{3} (\sigma_x + \sigma_y + \sigma_z).$$

$$\{S\} = \text{the deviatoric stress} = \{\sigma\} - \sigma_m [1 \ 1 \ 1 \ 0 \ 0 \ 0]^T$$

β = is a material constant which is given as:

$$\beta = \frac{2 \sin \phi}{\sqrt{3}} \frac{1}{(3 - \sin \phi)}$$

where:

ϕ = the input angle of internal friction.

The material yield parameter is defined as

$$\sigma_y = \frac{6c \cos \phi}{\sqrt{3} (3 - \sin \phi)}$$

where:

C = the input cohesion value.

It may be noted that, the Drucker-Prager yield criterion has two input parameters (ϕ and C).

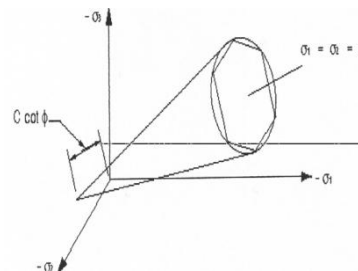


Fig1;Drucker- Prager and Mohr-Coulomb Yield Surfaces

III. FAILURE CRITERIA FOR BALLAST

The actual behavior and strength of ballast materials are very complex because they depend on many factors such as the physical and mechanical properties of the particles such as ballast size, air voids, friction between particle and the nature of loading. No single mathematical model can describe the strength of real

ballast materials completely under all conditions; so, simple models or criteria are used to represent the properties that are essential to the problem being considered.

(Willam and Warnke, 1975) developed a mathematical model capable of predicting failure for the solid cracking in tension and crushing in compression. In concrete applications, for example, the solid capability of the element may be used to model the concrete. Other cases for which the model is also applicable would be reinforced composites (such as fiberglass) and geological materials (such as rocks) (ANSYS,2007). Both cracking and crushing failure modes are accounted for. This model is represented by the following equation:

$$\frac{F}{f_c} - S \geq 0$$

where, F =function of principal stress state ($\sigma_{xp}, \sigma_{yp}, \sigma_{zp}$).

S= Failure surface expressed in terms of principal stresses and five input parameters (f_c', f_t', f_{cb}', f_1 and f_2).

f_c' = ultimate uniaxial compressive strength.

f_t' = ultimate uniaxial tensile strength.

f_{cb}' = ultimate biaxial compressive strength

f_1 = ultimate compressive strength for a state of biaxial compression superimposed on hydrostatic stress state (σ_h^a)

f_2 = ultimate compressive strength for a state of uniaxial compression superimposed on hydrostatic stress state (σ_h^a)

σ_h^a = ambient hydrostatic stress state.

The failure surface is separated into hydrostatic (change in volume) and deviatoric (change in shape) sections as shown in Figure (3-2). The hydrostatic section forms a meridional plane which contains the equisectrix $\sigma_1 = \sigma_2 = \sigma_3$, as an axis of revolution. The deviatoric section lies in a plane normal to the equisectrix (dashed line). The deviatoric trace is described by the polar coordinate (r, θ); where (r) is the position vector locating the failure surface with angle (θ). The failure surface is defined as:

$$f(\sigma_m, \tau_m, \theta) = \frac{1}{2} \frac{\sigma_m}{f_c'} + \frac{1}{r(\theta)} \frac{\tau_m}{f_c'} - 1 = 0$$

Where

σ_m and τ_m =average stress components defined as:

$$\sigma_m = \frac{1}{3} (\sigma_1 + \sigma_2 + \sigma_3) = \frac{1}{3} I_1$$

$$\tau_m^2 = \frac{2}{5} J_2$$

I_1 = first stress invariant

J_2 = second deviatoric stress invariant

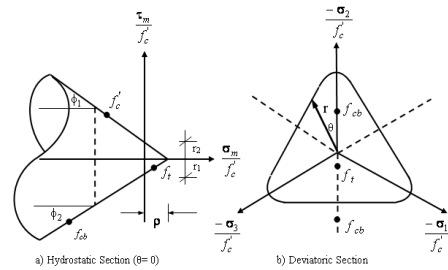


Fig2:Failure Surface (Chen, 1982)

IV. GEOMETRY AND MODEL CREATION

In actual field condition, the soil is usually of infinite extent both in horizontal and vertical directions. In the finite element idealization, the horizontal boundary of the soil blocks in the (x) and (y) directions. The dimensions of the soft soil considered in the analysis are (1000x400x500mm) for the length (in x-direction), width (in z-direction) and depth (in y-direction) respectively. All dimensions of soft soil layer have been kept constant for all analyses, while, the depth (thickness) of ballast layers is variable and depends on considered case (state).[2]

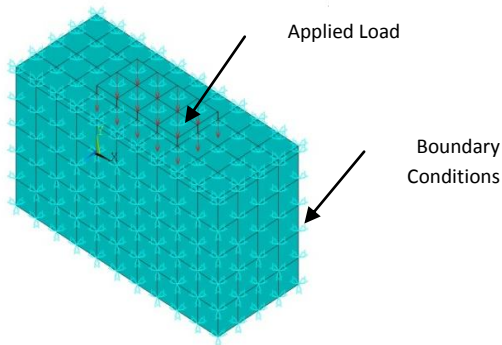
V. LOADING AND BOUNDARY CONDITIONS

Displacement boundary conditions (which represent the conditions at the interface of model) are needed to constrain the model to get a unique solution. To ensure that the model acts the same way as a real case, boundary conditions need to be applied at all sides of the model, and where the loadings exist. The word load in ANSYS includes boundary condition and external or internal applied force (different types of load available in ANSYS such as structural, thermal, magnetic, electric, fluid...). Show figure(1)The type of loading are used in this study is concentrated loads with different value. Due to load concentration on ballast elements, crushing of the ballast starts to develop in the elements located directly under the loads. Subsequently, adjacent ballast elements crushed within several load steps. As a result, the model shows a large displacement, solution diverged and finally, the finite element model fails prematurely. Therefore, to prevent this phenomenon, two techniques are used:-

- 1-Finer mesh is used under applied load.
- 2-Steel plates are used under load.

In this reserch, the second technique is adopted, and the employed boundary conditions are, as follows:-

1. Hinges, at the side of model in x and z-directions and, Rollers in y-directions.
2. Fixed at the bottom face of model (restrained the nodes in x, y and z-directions)



Fig(3)Boundary conditions and Loading of the Model

ModelsParameters The finite element models adopted in this study have a number of parameters, which can be classified into four categories:

- i- Soft soil property parameters, Table (1).
- ii- Ballast property Parameters, Table (2)
- iii-Geogrid property parameters, Table (3)
- iv- Steel plates property, Table (4)

Table (1) Soft Soil Property Parameters

Parameter	Definition	value	Note
C _u	Unrained shear strength (kPa)	9.0	Assumed
		25	
E	Elastic Modulus of Elasticity (MPa)	4.5	E=250C _u -500C _u *
		12.5	
v	Poisson's ratio	0.15	*
φ	Angle of Friction	0	-

* Das, (2006)

Table (2) Ballast Property Parameters

Parameter	Definition	value	Note
f _c	Ultimate Compressive Strength (MPa)	48	*
E	Elastic Modulus of Elasticity (MPa)	130	*
v	Poisson's ratio	0.45	*
β _c	Shear transfer Coefficient close	0.22	ANSYS,(2007)
β _o	Shear transfer Coefficient open	0.2	

* Iraq Railway Company

Table (3) Geogrid Property Parameters*

Parameter	Definition	value	Note
f _t	Peak tensile strength (N/mm)	13.5	*
E	Elastic Modulus of Elasticity (MPa)	25	*
v	Poisson's ratio	0.3	*
t	Thickness (mm)	3	Assumed

* Saudi Arabian stander organization (SASO) test method ISO10319

Table (4)Steel Plate Property Parameters

Parameter	Definition	value	Note
f _y	Ultimate tensile strength (MPa)	420	Assumed
E	Elastic Modulus of Elasticity (MPa)	200x10 ³	*
v	Poisson's ratio	0.3	*
t	Thickness (mm)	30	Assumed

*(ACI-318-08)

VI. ULTIMATE LOAD CAPACITY

Table (5-3) shows comparison between the ultimate loads of third group from the finite element analysis. For the first four models of this group, Table (5-3) shows that the presence of ballast layers of thickness (25, 50, 75 and 100mm) and reinforced with geogrid layer leads to an increase in load capacity for about (213%, 300%, 464% and 688%) for models (SGB-1, SGB-2, SGB-3 and SGB-4) respectively, while, the settlement decreases for about (59%, 53%, 36% and 10%) for the same models.

In other words, when the ballast layer is increased from (25mm) to (50, 75, 100mm) the load capacity increases for about (280%, 80% and 152%) for models (SGB-2, SGB-3 and SGB-4) respectively. Also, when the ballast layer is increased from (50mm) to (75 and 100mm), the load capacity increases for about (41% and 97%) for models (SGB-3 and SGB-4) respectively. While, increasing the ballast layer from (75mm) to (100mm) leads to increase the load capacity for about (40%) for model (SGB-4).

On the other hand, when the undrained shear strengths of untreated soil is increased (from 9 kPa to 25 kPa) instant with presence of geogrid layer and ballast layers of thickness (25, 50, 75 and 100mm), the modulus of elasticity increases, and the load capacity increases for about (107%, 107%, 164% and 227%) for the last four models of this group, (SGB-5, SGB-6, SGB-7 and SGB-8) respectively. Also, the settlement decreases for about (37%, 55%, 56% and 36%) for the same models.

In other words, when the ballast layer is increased from (25mm) to (50, 75, 100mm), the load capacity increases for about (28% and 58%) for models (SGB-7 and SGB-8) respectively. Also, when the ballast layer is increased from (50mm) to (75 and 100mm) the load capacity increased for about (28% and 58%) for models (SGB-7 and SGB-8) respectively. While, increasing the ballast layer from (75mm) to (100mm) leads to an increase in the load capacity for about (24%) for model (SGB-8). This means the value of undrained shear strengths and presence of geogrid

under the ballast layers represent an important parameters to improve soil and as a result, the load capacity increased. Also, increasing the value of undrained shear strengths from (9kPa) to (25kPa) lead to increase (improve) the carrying capacity of soft soil and as a result, the load transferred by ballast decreased.

Table (5) Ultimate Load and Maximum Settlement for Model

Mode 1	$(P_u)_R$ (kN)	P_u (kN)	$(P_u)_i / (P_u)_R$	$(S)_R$ (mm)	S (mm)	$(S)_i / (S)_R$
SGB-1	8.0	25	3.13	40	16.5	0.41
SGB-2		32	4.00		18.6	0.47
SGB-3		45	5.64		25.7	0.64
SGB-4		63	7.88		36	0.9
SGB-5	20.8	43	2.07	21	13.2	0.63
SGB-6		43	2.07		9.5	0.45
SGB-7		55	2.64		11	0.44
SGB-8		68	3.27		13.5	0.64

* $(P_u)_R$ = Ultimate Load of Untreated Soil for Two Undrained Shear Strength (S-1 & S-2)

In general, all models where geogrid layer incorporates with ballast layer demonstrate a pronounced increase in ultimate load, as compared to unreinforced models. This state is true due to the interlocking action between the geogrid and the ballast particles. The geogrid at this specific location will gradually being drawn into the soil generating a sliding action of the soft soil layer along the base of both ballast and geogrid at moderate displacements. Ultimately at large displacements the ballast particles will penetrate the geogrid apertures.

VII. LOAD-SETTLEMENT RELATIONSHIP

The relationship between the applied load (P) and the corresponding settlement (S) for the models of the third group (SGB-1, SGB-2, SGB-3, and SGB-4) and (SGB-5, SGB-6, SGB-7, and SGB-8) is constructed and compared with referencemodels (S-1 and S-2) as shown in Figures (4) and (5). The results demonstrate a substantial increase in the ultimate load with the increasing thickness of ballast due to the distribution of the applied load.

Fig (4) Load-Settlement Curve for models(1,2,3,4)and

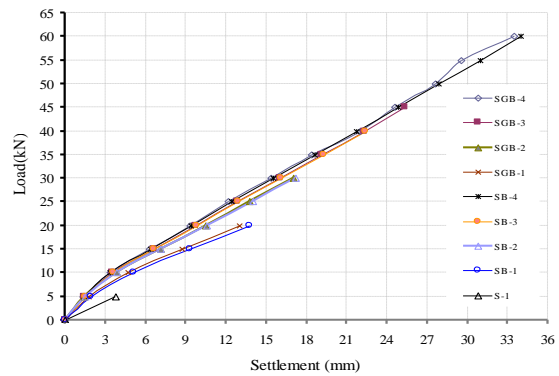
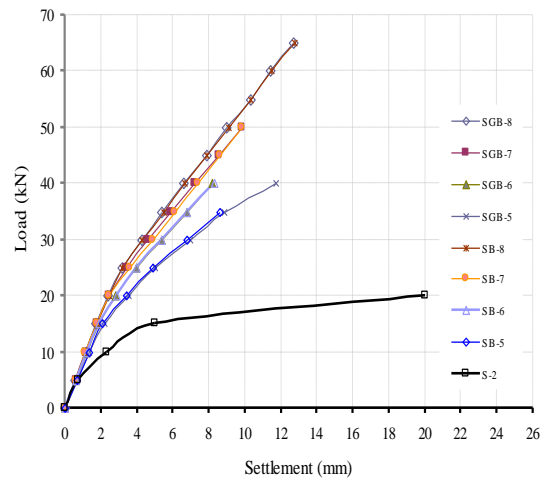
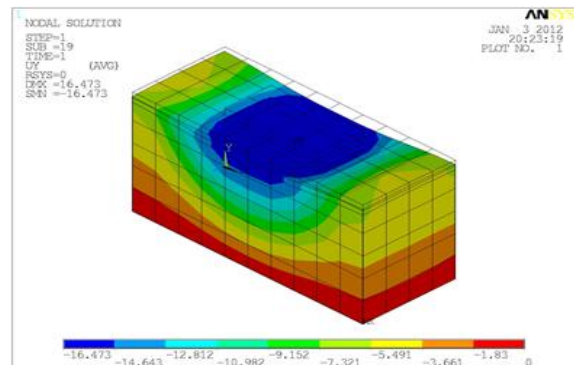


Fig (5) Load-Settlement Curve for models(5,6,7,8)and Untreated Model (S-2)

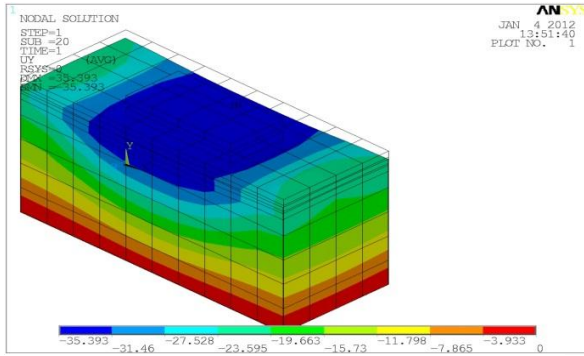


VIII. FAILURE MODE

The ANSYS program records a deflected shape pattern at each applied load step. Figures (6) to (13) show the failure modes developing for the models of treated models at the ultimate load. As shown in the figures, shear failure pattern appears underneath the loading location and ultimately at large displacements the ballast particles will penetrate the soft soil layer, and the failure takes place.



fig(6) failure model for treated soil SGB1



fig(7) failure model for treated soil SGB2

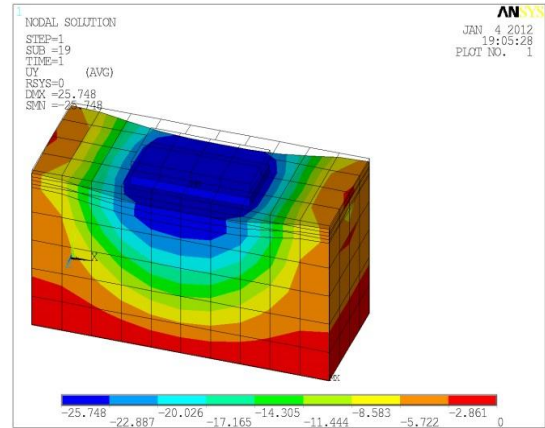


Fig (11) Failure Mode of Treated Soil Model SGB-6

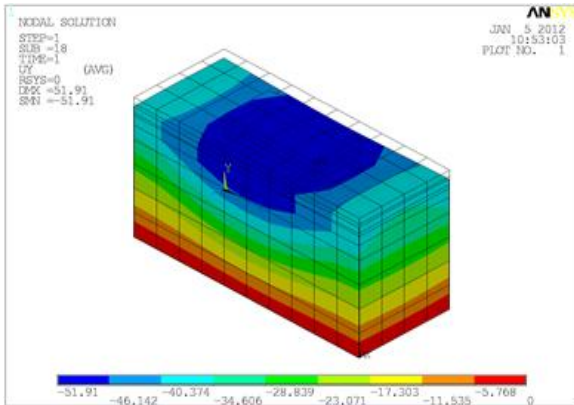


Fig (8) Failure Mode of Treated Soil Model SGB-3

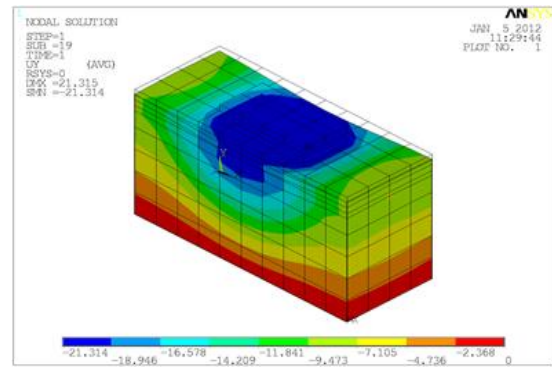


Fig (12) Failure Mode of Treated Soil Model SGB-7

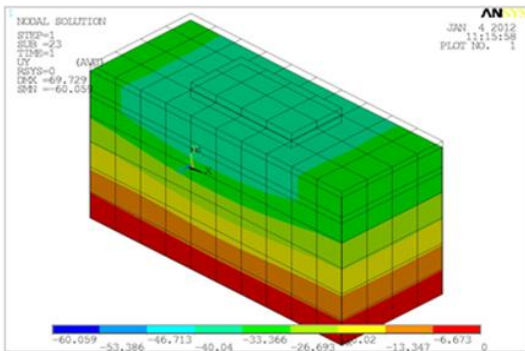


Fig (9) Failure Mode of Treated Soil Model SGB-4

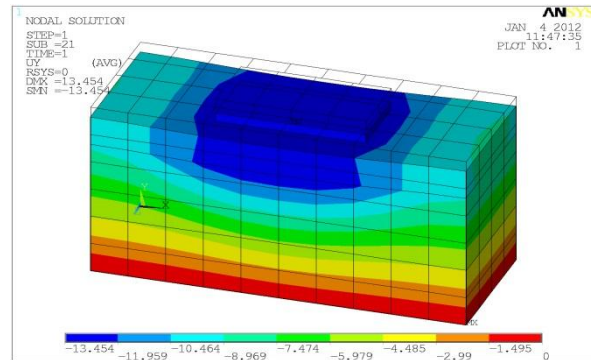


Fig (13) Failure Mode of Treated Soil Model SGB-8

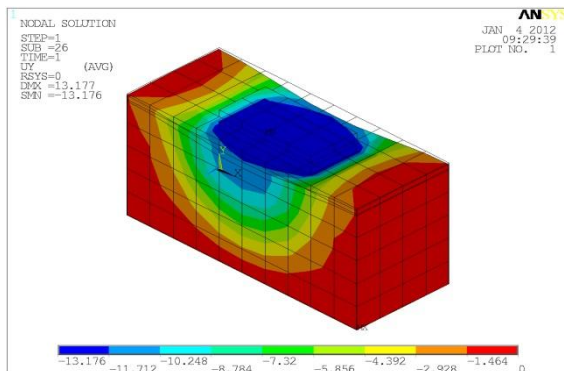


Fig (10) Failure Mode of Treated Soil Model SGB-5

Table (6) Summary of Finite Element Analysis Results

Group	Model	C_u (kPa)	P_u (kN)	Settlement (mm)	$(P_u)_i / (P_u)_R$
G-1	S-1*	9	8.0	40	-
	S-2*	25	20.8	21	2.6
G-2	SGB-1	9	25	16.5	3.13
	SGB-2		32	18.6	4.00
	SGB-3		45	25.7	5.64
	SGB-4		63	36	7.88
	SGB-5	25	43	13.2	2.07
	SGB-6		43	9.5	2.07
	SGB-7		55	11	2.64
	SGB-8		68	13.5	3.27

*Reference Models

IX. CONCLUSIONS

Based on the results obtained from the finite element analysis for the improvement of soft soil reinforced with or without geogrid, the following conclusions are presented:-

1-Theoretical solution using ANSYS Finite Element program can be adopted in the evaluation of loads and the amount of settlement for the soil layers beneath the railway lines as well as Ballast. The program gives good correlation and a sufficient degree of convergence in behavior.

2-The vertical displacement (settlement) under the applied load decreases with the increase of shear strengths (C_u). Increasing the soil shear strength improves the load carrying capacity significantly. This enhancement starts even from the lower load and increases with increase in load.

3-The vertical displacement (settlement) under the applied load decreases with the increase of Modulus of Elasticity (E) of the soil. Increasing soil modulus improves the load carrying capacity significantly.

4-The maximum vertical displacement under the applied load decreases with the increasing of the ballast thickness.

5- Presence of geogrid layers leads to reduce the vertical displacement (settlement), while the corresponding load carrying capacity increases significantly. The uniformly oriented geogrid and its ability to improve soft soils cause an increase in the load carrying capacity. This is combined with the ability of ballast layer to sustain larger compressive force at advanced stages of loading.

REFERENCES

[1] Abbawi, Z.W.S., (2010), "Evaluation of Improvement Techniques for Ballasted Railway Track Model Resting on Soft Clay", Ph.D. Thesis, University of Technology, Iraq.

[2] Drucker, D.C., and Prager, W., (1953), "Soil Mechanics and Plastic Analysis of Limit Design", Q. Appl. Math
 [3] Das, B. M., (2006), "Principles of Geotechnical Engineering" 5th Edition Nelson, a division of Thomson Canada.
 [4] ACI Committee 318, "Building Code Requirements for Structural Concrete", (ACI 318-08) and Commentary (ACI 318R-08). American Concrete Institute, Farmington Hills, MI, 2008, pp. 465.
 [5] ANSYS, "ANSYS Help", Release 11, Copyright 2007.
 [6] Iraq Railway Company "Ballast Specification"
 [7] Chen, W., "Plasticity in Reinforced Concrete", McGraw-Hill Book Company, pp. 592, U.S.A, 1982.